PROPULSIVE CHARACTERISTICS OF BIOMORPHING FOILS IN GROUND EFFECT

Cheolheui Han*, Hakjin Lee, Jinsoo Cho*****
***Konkuk University, **Sindorico, *** Hanyang University**

Keywords: *Biomorphing Foil, Ground Effect, Unsteady Panel Method*

Abstract

The study on the unsteady aerodynamic analysis of biomorphing airfoils is important in its applications to the aerial and hydro robots. The wake patterns and thrust characteristics of biomorphing airfoils are investigated using an unsteady panel method. To trace complicated wake shapes behind airfoils, a core addition scheme, a vortex core model, and the fourth order Runge-Kutta convection scheme are employed. Present results are verified by comparing them with flow visualization, exact solution and published computed results.

1 Introduction

Mimicking small birds or insect has led to the development of small scale flying robots [1]. The flapping-wing mechanism to generate lift to overcome its weight has the advantage that when the size decreases flapping-wing flight is much more efficient than fixed-wing flight [2]. The basic understanding of propulsion mechanism of fish and cetaceans can be utilized to enhance the current technology [3].

The basic propulsion mechanism of flapping foils has been known that the shed wakes from the foils' trailing edges are developed as the staggered array of vortices with reverse direction of rotation to a von Karman vortex street (known as the Knoller-Betz effect)[4-6]. Jones *et al*.[6] showed that the formation and evolution of unsteady wakes is fundamentally an inviscid phenomenon over a broad range of Strouhal numbers. The tails of some of the fastest swimming animals resemble high aspect ratio foils, which has led to the theoretical and numerical studies [3].

When multiple foils operate side by side, the vortex-to-vortex interaction can results in a drag wake and the deterioration of propulsive performance [3]. The strong interaction between foils close to each other produces the drag-wake-like flow fields. However, two foils flapping in antiphase show that the strong interaction can produce larger thrust than other configurations [7]. This phenomenon is similar to the biomorphing foil propulsion near the ground. However, there has not much published literature on this phenomenon.

The purpose of this paper is to investigate the wake patterns and propulsive characteristics of biomimetic foils moving near the ground. To accurately simulate the closely coupled interacting wakes between foils, a core addition scheme and a vortex core model are combined. A time history of aerodynamic coefficients of a flapping foil is compared with other numerical data.

2 Unsteady Panel Method

Generally, two coordinate systems(one is a body-fixed coordinate system, and the other is the ground-fixed coordinate system) are used to simulate the foils moving through the fluid. The foils of creatures such as insects or birds in nature are moving under the significant influence of the viscosity. However, man-made foils can be fly at higher velocities than the foils of creatures. Thus, it is assumed that the viscous effect is confined within a thin boundary layer. To simplify the complicated unsteady problems of morphing and oscillatory motions combined,

it is further assumed that the flow is inviscid, incompressible and irrotational over the entire flow field, excluding the foils' boundaries and their wakes.

The isentropic flow around the deforming foils can be solved using the continuity equation coupled with energy equation. Mass should be conserved regardless of the coordinate systems. Therefore,

$$\nabla^2\Phi = 0 \qquad (1)$$

(in a body-fixed coordinate system)

The foils deforming body surface is discretized into N equal length panel elements. The vorticity on each element is considered to be linear. As shown in Fig. 1, the vorticity of linear strength on each element is represented as

$$\gamma(x) = \gamma_j + \gamma_{j+1}(x - x_{j+1}) \qquad (2)$$

The wake is represented by free vortices which deform freely by the assumption of a force-free position during the simulation. These free vortices are connected to the bound vortices at the trailing edge of the foil through the Kutta condition. The strengths of the elementary solutions are obtained by enforcing boundary conditions as follows.

A. The flow disturbance, due to the foil's motion through the fluid, should vanish far from the plates. This boundary condition can be satisfied automatically by using the vortices as the singularity distributions.

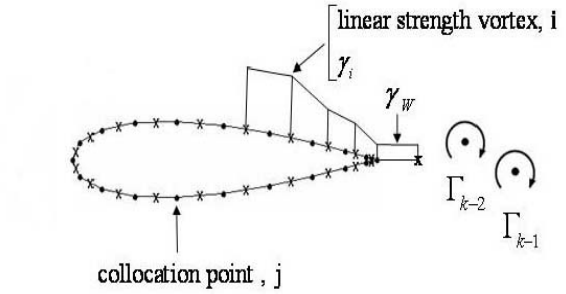

Fig. 1 Nomenclature of the Present Method.

B. Zero normal flow across the foils' solid boundaries. The continuity equation (1) does not directly include time-dependent terms. Time dependency is introduced through the modification of "zero normal flow on a solid surface" and the use of the unsteady Bernoulli equation. The kinematic velocity ($\vec{v}$) is given as follows,

$$\vec{v} = -[\vec{V}_0 + \vec{v}_{rel} + \vec{\Omega}\times\vec{r}] \qquad (3)$$

where $\vec{V}_O$ is the velocity of the body-fixed system's origin, $\vec{r}$ = (x, y, z) is the position vector of the foil's surface the body-fixed system, $\vec{\Omega}$ is the rate of rotation of the body-fixed coordinate system with respect to the ground-fixed coordinate system. The additional relative motion within the body-fixed coordinate system is represented as $\vec{v}_{rel}$. The zero-velocity normal to a solid surface boundary in the body-fixed frame becomes

$$(\nabla\Phi - \vec{V}_0 - \vec{v}_{rel} - \vec{\Omega}\times\vec{r})\cdot\vec{n} = 0 \qquad (4)$$

where $\vec{n}$ is the normal to the body's surface, in terms of the body-fixed coordinates (x,y).

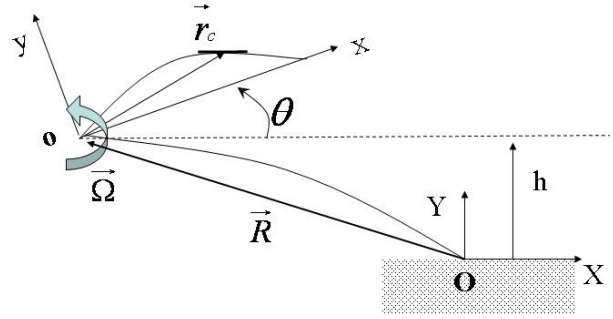

(a) coordinate systems

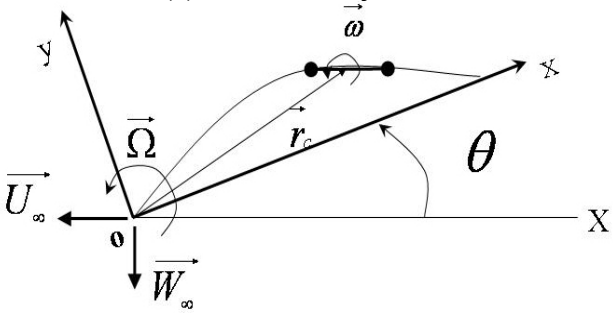

(b) nomenclature of relative velocities

Fig. 2 Nomenclature for the Unsteady Motion of a Morphing Foil.

For a foil in heave oscillation near the ground, the kinematics of the foil can be represented as follows

$$\overrightarrow{R(t)} = (X(t), Y(t)) \qquad (5)$$

$$X(t) = -U_\infty t$$
$$Y(t) = -W_\infty t + h_o \cos(\omega_h t - \phi) + h$$

$$\overrightarrow{V_O} = -U_\infty \vec{i} - \{W_\infty + h_o \omega_h \sin(\omega_h - \phi)\}\vec{i}$$

where h is the distance between the origin of the body-fixed coordinate system and the ground, ho is the heaving amplitude, ω_h is the heaving oscillation frequency. Both U_∞ and W_∞ represent the left moving and sinking velocity components of $\overrightarrow{V_O}$, respectively.

The relative velocity, $\overrightarrow{v_{rel}}$, is zero when the foil is rigid. When the foil deforms, $\overrightarrow{v_{rel}}$ is the relative velocity of the foil surface.

$$\overrightarrow{v_{rel}} = \overrightarrow{dr_c} / dt + \vec{\omega} \times \vec{r_c} \qquad (6)$$

Fulfilling the boundary condition on the surface requires that, at each collocation point, the normal velocity component will vanish and we can write Eq. (4) as

$$\left(\sum_{j=1}^{N+1} A_{ij}\gamma_i + A_{iN+2}\gamma_w \right) \cdot \mathbf{n}_i = -\left(\mathbf{V}(t) + \mathbf{V}_{iw}\right) \cdot \mathbf{n}_i \qquad (7)$$

on the foil for i=1,2,...., N (5)

where the influence matrix element A_{ij} represents the normal velocity component at a control point, i, by the vortex (having a unit circulation) at the panel element, j. The elements a_{ij} are functions of geometry. Γ_j is the unknown circulation of the point vortex representing the vorticity of the panel element, j. q_i represents the normal velocity component induced at control point i by the starting vortex and its image. V_{wi} is the velocity induced by the wake vortices and their images whose positions and circulations are known. At the beginning, V_{wi} is zero. The calculation begins at t = Δt and the wake at this moment consists of a single vortex, Γ_c.

C. Kelvin condition. The use of the Kelvin condition that the circulation around a fluid curve enclosing the plates and their wakes are conserved, will supply an additional equation.

D. The unsteady Kutta condition. This condition at the trailing edge of a plate is satisfied by shedding the vorticity generated at the trailing of a plate at the local fluid particle velocity.

E. Continuous pressure across the wake. This condition is fulfilled with convecting wakes downstream at the local fluid particle velocity.

To find the solutions of Eq. (5), an initial condition describing the position of the wake and its vorticity must be prescribed. At each time step, a newly shed starting vortex is fixed at a point l/4 l behind a plate's trailing edge as required by the unsteady Kutta condition. All the circulation strengths are determined including the effects of their images by Gauss elimination. At the end of each time step, the shed vortex is convected downstream to its new position at the local fluid particle velocity. The procedure is repeated for any desired number of time steps.

Since the wake is force-free, each vortex representing the wake must move with the local flow velocity. The local flow velocity is the result of the velocity components induced by the wake and the plate. The 4th-order Runge-Kutta method is used for the convection scheme.

In the body fixed frame, thrust (or drag) is calculated using the momentum conservation theorem.

$$T(or\ D) = \rho \int_{-\infty}^{\infty} V(y)\left[V(y) - U_\infty\right] dy \qquad (8)$$

where $V(y)$ is the velocity profile at the cross section behind a chord length from the plate's trailing edge.

The mean camberline of a flexible foil can be represented as a following equation.

$$f(x_c, t) = H(x_c)\cos\left(\frac{\omega}{U_\infty} x_c - \omega t\right) \qquad (9)$$

$$H(x_c) = A\left[(x_c - c)^2 - b^2\right]$$

The time variation of the mean camberline as represented in Eq. (9) has the form of the traveling wave (See Fig. 3).

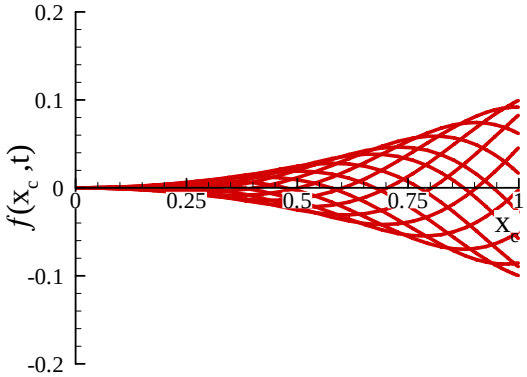

Fig. 3 Time Variation of the Mean Camberline.

3 Results and Discussions

Fig. 4 shows the induced drag coefficients of a foil undergoing heaving oscillation. Present method is validated by comparing the present result with the computed result by CFD[8]. Present result for dxw=0.05 is in good agreement with the CFD result[8].

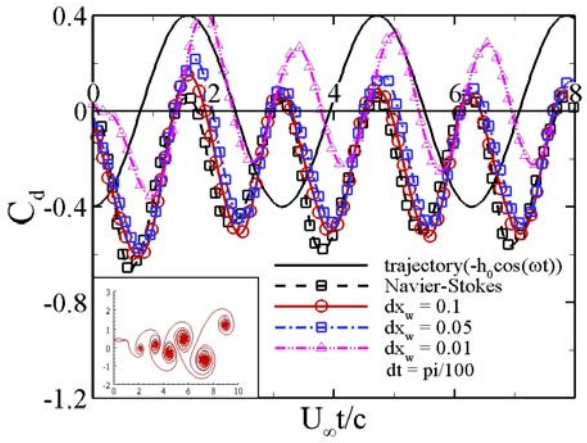

Fig. 4 Time History of the Induced Drag Coefficient.

Fig. 5(a) shows the computed wake patterns behind heaving foils using the CFD[8]. Fig. 5(b) also shows the computed wake patterns of the foil and its image using the present method. It can be deduced from the figure that the present result is in good agreement with the CFD results[8].

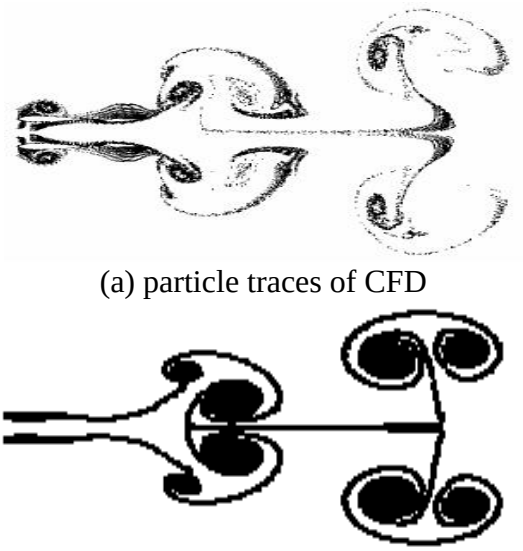

(a) particle traces of CFD

(b) present method

Fig. 5 Comparison of Wake pattern behind Heaving Foils for k=2, h_0=0.4, and y_0=1.4.

Fig. 6 and 7 shows the wake pattern behind a morphing foil and its thrust coefficients when the foil is moving at a constant speed near the ground. Lai and Platzer[9] investigated the wake shapes behind a plunging foil. They found that, when the vortex patterns in a mushroom form is pointing upstream, the drag is producing. The vortex on the upper part of the vortex street has the clockwise rotation direction and the vortex on the lower part of the street has the clockwise rotation direction. This vortex pattern is called as von Karman vortex street. When the mushroom head points upward, then the foil produces zero drag (or zero thrust). The thrust is produced when the mushroom head points downstream. In this case the rotation direction of the von Karman vortex street is reversed and these vortex streets are called as reverse von Karman street. The vortex patterns in Fig. 6 show that the mushroom head points downstream. When the foil is moving forward in close proximity to the ground, the mushroom head changes the pointing direction from downstream to upstream. As shown in Fig. 7, the value of the time-averaged thrust coefficient decreases with the foil moving closer to the ground.

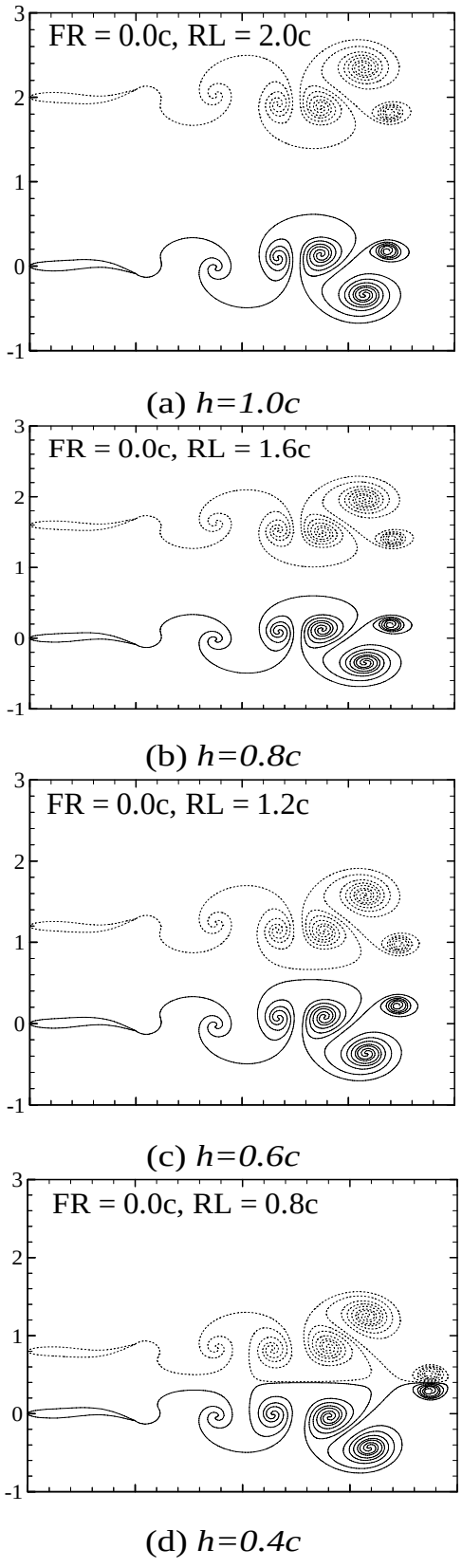

Fig. 6 Wake Patterns Behind a Foil Near the Ground.

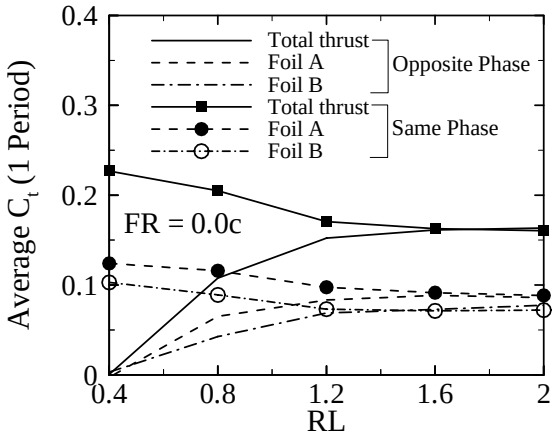

Fig. 7 Ground Effect on the Thrust Generation.

4. Summary

An unsteady panel method is developed with a boundary condition that treats the relative velocity components caused by the deformation of the foil. For the present mean camberline change of the foil, the thrust of the foil in ground effect is smaller than that of the foil out of the ground effect. It can be deduced that the present result can be applied to the unsteady aerodynamic analysis of a biomorphing foil in ground effect.

Acknowledgements

This work was supported by Grant No. (R01-2005-000-10310-0) from the Basic Research Program of the Korean Science and Engineering Foundation. This work was also supported by Korea Research Foundation Grant (KRF - 2004 - 005 - D00045, KRF - 2005 – 206 -D00007).

References

[1] Yan, J., Wood, R., Avandhanula, S., Sitti, R., and Fearing, R.S., Towards Flapping Wing Control for a Micromechanical Flying Insect, *IEEE International Conference on Robotics and Automation*, The IEEE Robotics and Automation Society, Seoul Korea, May 21-26, pp. 3901-3908, 2001.

[2] Mueller, T. J., *Fixed and Flapping Wing Aerodynamics for Micro Air Vehicle Applications*, AIAA, Inc., 2001, Chap. 1.

[3] Triantafyllou, M. S., Techet, A.H., Hover, F.S., Review of Experimental Work in Biomimetic Foils, *IEEE Journal of Oceanic Engineering*, Vol. 29, No. 3, July, 2004.

[4] Knoller, R., Die Gesetze des Lufwiderstandes, *Flug- und Motortechnik(Wien)*, Vol. 3, No. 21, pp. 1-7, 1909.

[5] Betz, A., Ein Beitrag zur Erklarung des Segelfluges, *Zeitschrift fur Flugtechnik und Motorluftschiffahrt*, Vol. 3, pp. 269-272, Jan. 1912.

[6] Jones, K. D., Dohring, C. M., and Platzer, M. F., Wake Structures Behind Plunging Airfoils: A Comparison of Numerical and Experimental Results, *AIAA Paper 96-0078*, Jan. 1996.

[7] Han, C. and Cho, J., Unsteady Aerodynamics Analysis of Flat Plates in Pitch Oscillation," *AIAA Journal*, Vol. 44, No.6, pp.1121-1126, 2006.

[8] Tuncer, I. H. and Mustafa Kaya, Thrust Generation Caused by Flapping Airfoils in a Biplane Configuration, *Joural of Aircraft*, Vol. 37, No. 3, 2003.

[9] Lai, J. C. S., and Platzer, M. F., Jet Characteristics of a Plunging Airfoil, *AIAA Journal*, Vol. 37, No. 12, pp. 1529-1537, 1999.

[10] Kagemoto, H., Wolfgang, M. J., Yue, D. K. P., M. S., Triantafyllou, Force and Power Estimation in Fish-Like Locomotion Using a Vortex-Lattice Method, *Journal of Fluids Engineering*, Vol. 122, pp. 239-253, 2000.

[11] Lighthill, M. J., *Collected Papers of Sir James Lighthill*, edited by M. Yousuff Hussaini, Volume IV, Oxford University Press, New York, Chap. 77, 1997.